HEPSY-93-4
Fermilab Library
0 1160 0031463 2

HEPSY 93-4
Sept., 1993

# Hadronic $B$ Decays

Sheldon Stone

*Physics Department, Syracuse University*
*Syracuse, New York 13244-1130*

C93/07/06.1

FERMILAB
OCT 11 1993
LIBRARY

*Invited talk presented at "Proceedings for the 5th International Symposium on Heavy Flavour Physics," Montreal, Canada, June 1993*

HEPSY 93-4
Sept., 1993

# Hadronic $B$ Decays

Sheldon Stone

*Physics Department, Syracuse University*
*Syracuse, New York 13244-1130*

**Abstract**

Branching ratios of two-body hadronic $B$ decays to charm or charmonium mesons are presented as well as polarizations in the vector-vector final states $D^{*+}\rho^-$ and $\psi K^*$. Factorization is shown in work well in final states containing a $D^{*+}$ and a light hadron, $\pi^-$, $\rho^-$, or $a_1^-$. Assuming factorization in $DD_s^-$ modes, a value of $f_{D_s}$ of 315±46 MeV is derived in conjunction with the CLEO measurement of $\Gamma(D_s^+ \to \mu^+\nu)/\Gamma(D_s^+ \to \phi\pi^+)$. The BSW parameters, $a_1$ and $a_2$ are derived from the data, with values $a_1 = 1.07 \pm 0.04 \pm 0.03 \pm 0.09$, and $a_2 = 0.27 \pm 0.01 \pm 0.01 \pm 0.02$. The relatve sign is positive, opposite to that found in charm decay.

*Invited talk presented at "Proceedings for the $5^{th}$ International Symposium on Heavy Flavour Physics," Montreal, Canada, June 1993*

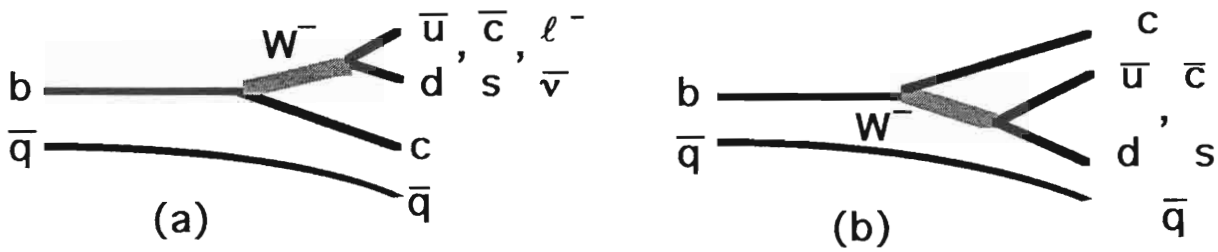


Figure 1: (a) The charged current spectator diagram for $B$ decays. (b) The "color suppressed" spectator diagram.

# 1 Introduction

At the parton level most $B$ decays can be described via the diagrams shown in Fig. 1. Other rare diagrams, especially those which don't produce charm, are expected to contribute only small amounts. These include $b \to s\gamma + sg$ which is within the range of 0.1% to 1% [1], and the $b \to u$ transisition, which is known to be about 1% [2]. The semileptonic decays, which can occur via Fig. 1(a), account for only about 20% of $B$ decays [2]. Since most of the $B$ decay rate is into hadronic channels, it is of no small importance to understand hadronic $B$ decays. Furthermore, in order to precisely extract the CKM parameters $V_{ub}$ and $V_{cb}$ it is necessary to use QCD based theoretical models, even in semileptonic decays. It is possible to check these models in hadronic decays adding the assumption of factorization.

In this paper I use the $D$ and $D^*$ branching ratios determined by CLEO and shown in Table 1. This approach is adopted because there is a large reduction of the CLEO systematic error in their $B$ branching ratios. It should be kept in mind, however, that most of the CLEO results presented here are preliminary.

Table 1: $D$ and $D^*$ Branching Ratios from CLEO

| Mode | $\mathcal{B}$ (%) |
|---|---|
| $D^{*+} \to \pi^+ D^0$[3] | $68.1 \pm 1.6$ |
| $D^{*0} \to \pi^0 D^0$[3] | $63.6 \pm 4.1$ |
| $D^0 \to K^- \pi^+$[4] | $3.91 \pm 0.08 \pm 0.17$ |
| $D^+ \to K^- \pi^+ \pi^+$[4] | $10.0 \pm 1.0 \pm 1.2$ |

# 2 Two-Body Decays

## 2.1 Introduction

Since many-body hadronic decays have thus far been too difficult describe theoretically, we will try to understand two-body decays. The simple spectator decay diagram shown in Fig. 1(a) can form two-body decays when the virtual $W^-$ transforms into a $\bar{u}d$ or $\bar{c}s$ pair, these pairs form a single hadron and the $c$ quark and spectator antiquark also form a single hadron. Hard gluon corrections lead to an additional diagram, shown in Fig. 1(b), called the "color suppressed" diagram, since the color of the quarks from the virtual $W^-$ must match the color of the intial $b$-quark. The existence of this diagram has been proven by observation of $B \to \psi K$ decays.

## 2.2 Two-body Branching Ratios

There is new CLEO data on exclusive $B$ decays. A potpourri of $B$ candidate mass spectra are shown in Fig. 2. The branching ratios are given in Table 2. All final state $D^0$'s are found in three modes, $K^-\pi^+$, $K^-\pi^+\pi^0$, and $K^-\pi^+\pi^+\pi^-$, while the $D^+$ is found only in $K^-\pi^+\pi^+$. These results are so much more precise than previous ones that they supersede all past measurements [5]. In computing these numbers it is assumed that there is equal charge and neutral $B$ production.

Table 2: Exclusive Two-body $B$ Branching Ratios (%)

| Mode | # of events | $\mathcal{B}(\%)$ |
|---|---|---|
| $B^0 \to D^{*+}\pi^-$ | 73± 9 | 0.27±0.04±0.04 ± 0.01 |
| $D^{*+}\rho^-$ | 73±10 | 0.74±0.11±0.13 ± 0.03 |
| $D^{*+}\pi^-\pi^-\pi^+$ † | 43±9 | 0.66±0.15±0.09 ± 0.05 |
| $D^+\pi^-$ | 76±10 | 0.22±0.03±0.02 ± 0.03 |
| $D^+\rho^-$ | 86±11 | 0.62±0.08±0.08 ± 0.09 |
| $B^- \to D^{*0}\pi^-$ | 93±12 | 0.50±0.06±0.07 ± 0.04 |
| $D^{*0}\rho^-$ | 92±12 | 1.41±0.19±0.29 ± 0.11 |
| $D^0\pi^-$ | 302±22 | 0.47±0.03±0.05 ± 0.02 |
| $D^0\rho^-$ | 209±19 | 1.07±0.10±0.16 ± 0.04 |

† The three pion mass is required to be between 1.0 GeV and 1.6 GeV consistent with an $a_1$ meson. (If the final state is pure $a_1$, the branching ratio for $D^*a_1^-$ is twice that quoted for $D^*\pi^-\pi^-\pi^+$.)

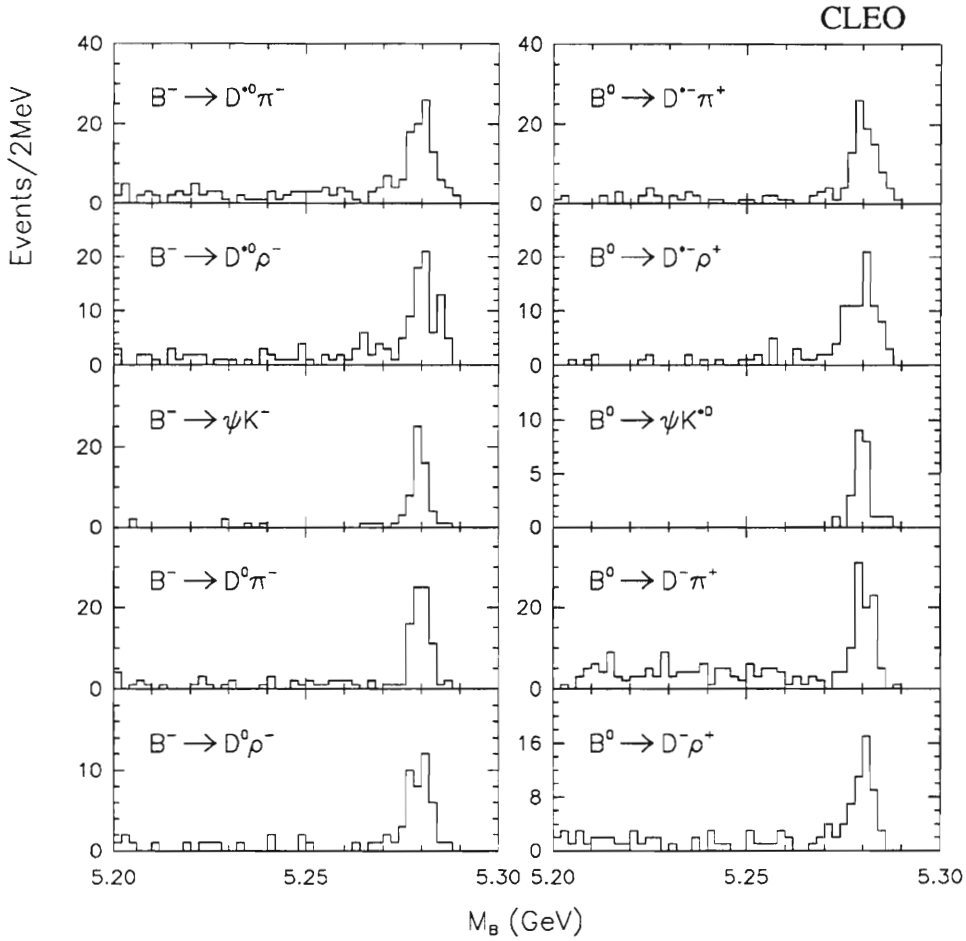


Figure 2: $B$ candidate mass spectra in several different decay modes. See ref. [9] for a description of the selection procedures.

Two systematic errors are quoted on the branching ratios. The first includes contributions from background shape ($\sim 5\%$), Monte Carlo statistics ($2-4\%$), and the uncertainty in the modeling of the tracking and $\pi^0$ detection efficiencies which depend on the multiplicity of the decay mode, while the second is due to errors on the $D^+ \to K^-\pi^+\pi^+$ ($\pm 14\%$) and $D^0 \to K^-\pi^+$ ($\pm 2.7\%$) absolute branching ratios.

In the cases of the $\pi^-\pi^0$ final states, the branching ratios have been entered as if the final states were pure $\rho^-$. For the $D^0\rho^-$ and $D^+\rho^-$ final state this assumption can be checked by looking at both the distributions in $\pi^-\pi^0$ mass and helicity angle, $\theta$, which is the angle of the $\pi^+$ in the $\pi^-\pi^0$ rest frame with respect to the $B$ direction in this rest frame. Since both the intial state $B$ and the final state $D$ are spinless, the spin-1 $\rho$ must follow a $cos^2\theta$ distribution. The data are consistent with pure $cos^2\theta$ as can be seen in Fig. 3. In the $D\rho^-$ modes the $\pi^-\pi^0$ mass distributions (not shown)

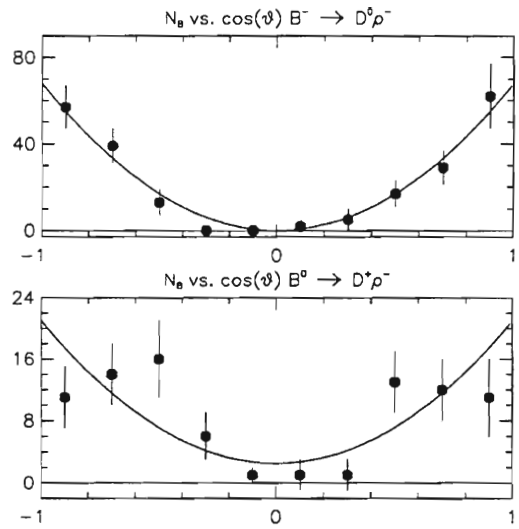


Figure 3: The $\rho^-$ helicity angle distributions for (a) $B^- \to D^0\rho^-$ and for (b) $\overline{B}^0 \to D^+\rho^-$. A subtraction has been performed to account for background in $B$ signal region by using low $B$ mass candidates.

are consistent with the expectations of pure $\rho^-$, as are the mass distributions in the $D^*\rho^-$ modes shown in Fig. 4.

The $D^{*+}\pi^+\pi^-\pi^-$ $B$ candidate mass plot is shown in Fig. 5(a). Here the three pion invariant mass is required to be consistent with the $a_1$ mass, i.e. to be in the interval $1.0 < \pi^-\pi^-\pi^+ < 1.6$ GeV. In order to show that this signal is dominantly $a_1$, we show the the Monte Carlo expectation of the three pion mass spectrum if it is pure $a_1$ in Fig. 5(b), or $D^*\rho^0\pi^-$ phase space in Fig. 5(c), and for the data in Fig. 5(d), where no restriction is placed on the three pion mass, but the events are required to be in the $B$ mass peak. A subtraction has been performed to account for background in $B$ signal region by using low $B$ mass candidates (5.2-5.6 GeV).

## 2.3 Factorization

### 2.3.1 Branching ratio tests

One approach to analysing two-body hadronic decays of $B$ mesons is to assume that the decay amplitude can be written as a product of two currents, as is done for semileptonic decays [6]. For example, $B \to D^*\ell\nu$ is given by $\langle D^*|J_\mu|B\rangle \times \langle\nu|\gamma_\mu(1-\gamma_5)|\ell\rangle$. In the case of two-body hadronic decays the leptonic term is replaced by a

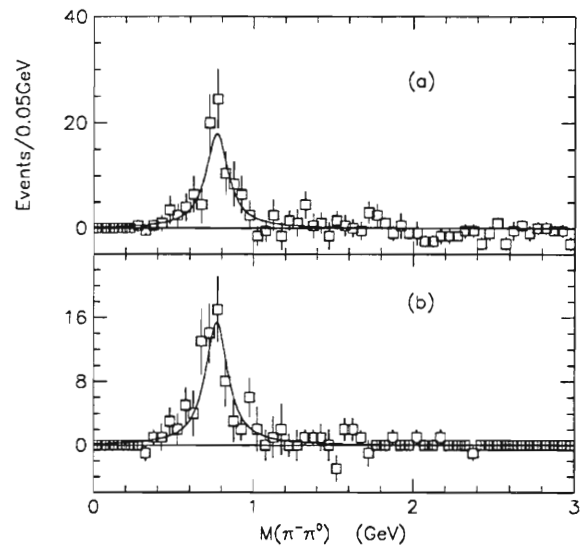


Figure 4: The $\pi^-\pi^0$ invariant mass distributions for for the reactions (a) $\overline{B}^0 \to D^{*+}\pi^+\pi^0$ and (b) $\overline{B}^0 \to D^{*0}\pi^+\pi^0$. A low $B$ candidate mass sideband subtraction has been made. The curves are fits to the data of a Breit-Wigner $\rho^-$ signal shape.

hadronic term. For $B \to D^{*+}\pi^-$ the amplitude is given by $\langle D^{*+}|J_\mu|B\rangle \times \langle 0|A_\mu|\pi^-\rangle$. This approach is called factorization, and is applicable in situations where the only the simple spectator diagram is allowed. Simple inspection shows that it is impossible to produce the $D^{*+}\pi^-$ final state from the color suppressed diagram.

Quantitative checks of factorization can be performed by comparing to the relevant semileptonic decay (see Fig. 1(a).) If factorization is correct, we have for the decay of a $\overline{B}^0$ to a $D^{*+}$ and a hadron $h^-$

$$\frac{\Gamma\left(\overline{B}^0 \to D^{*+}h^-\right)}{\frac{d\Gamma}{dq^2}\left(\overline{B}^0 \to D^{*+}\ell^-\overline{\nu}_\ell\right)\Big|_{q^2=m_h^2}} = 6\pi^2 c_1^2 f_h^2 |V_{ij}|^2, \tag{1}$$

where $|V_{ij}|$ is the CKM matrix element, $c_1$ is a hard gluon correction [7], and $f_h$ is the meson decay constant, whose magnitude is governed by the size of the coupling to the virtual $W$. For $h^- = \pi^-$, for example, $f_h$ is calculated from the measured $\pi^- \to \mu^-\nu$ decay rate [9].

The denominator in equation (1) has been studied by Bortoletto and Stone (see Fig. 6) [8]. Table 3 shows the evaluation of the left side of equation (1) called $R_{\rm exp}$ and the right side called $R_{\rm theor}$, for three reactions. Factorization works very well in the case of $\pi^-$ and $\rho^-$, while the $a_1$ situation is less clear, due to the large error.

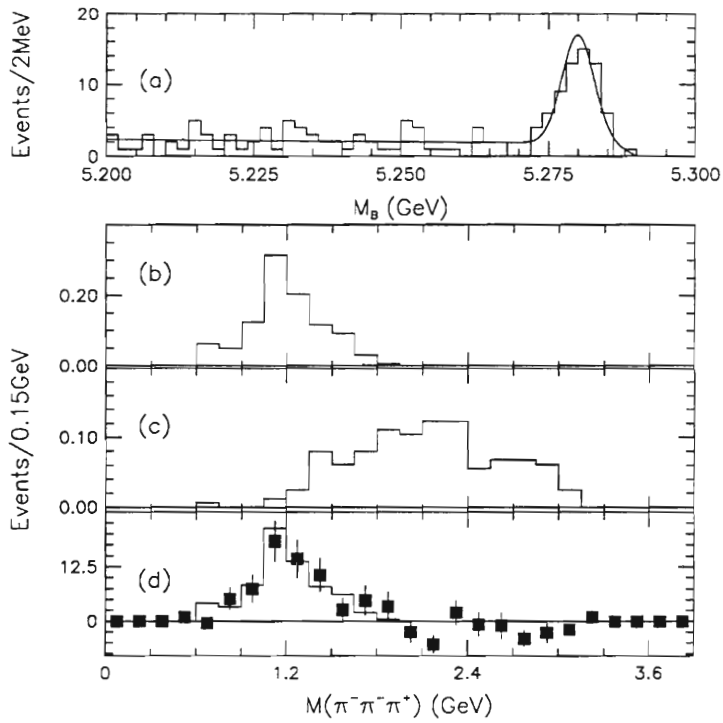


Figure 5: (a) The $B$ candidate mass plot for $D^{*+}\pi^+\pi^-\pi^-$, where the three pion mass is between 1.0 and 1.6 GeV. (b) Monte Carlo expectation of the the three pion mass for pure $a_1$. and for (c) pure $\rho^0\pi^-$. In (d) the data, uncut on three pion mass, are compared with the Monte Carlo expectation for pure $a_1$.

Table 3: Comparison of $R_{\rm exp}$ and $R_{\rm theor}$

| Mode | $R_{\rm exp}$ (GeV$^2$) | $R_{\rm theor}$ (GeV$^2$) | $f_h$ (MeV) |
|---|---|---|---|
| $\bar{B}^0 \to D^{*+}\pi^-$ | $1.2 \pm 0.2$ | $1.2 \pm 0.2$ | 131.7$\pm$ 0.2[9] |
| $\bar{B}^0 \to D^{*+}\rho^-$ | $3.0 \pm 0.4$ | $3.3 \pm 0.5$ | 215$\pm$4[10] |
| $\bar{B}^0 \to D^{*+}a_1^-$ | $4.3 \pm 1.1$ | $3.0 \pm 0.5$ | 205$\pm$16[11] |

### 2.3.2 Polarization tests

Factorization can also be tested when a $\overline{B}^0$ decays into a $D^{*+}$ and another vector meson, by comparing measured polarization of the $D^{*+}$ (and the other vector meson) to the polarization in $D^{*+}\ell^-\overline{\nu}_\ell$ decays. Unfortunately, the polarization has not as yet been well measured in the semileptonic channel, so the theoretical predictions shown in Fig. 6 for the longitudinal, $\Gamma_L$, and transverse, $\Gamma_T$, components of the polarization

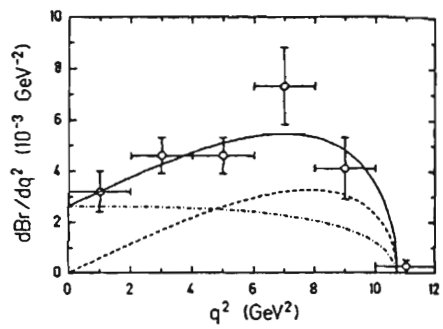


Figure 6: The $q^2$ distribution for $\overline{B}^0 \to D^{*+}\ell^-\bar{\nu}_\ell$ from an average of CLEO and ARGUS data. The curves show the theoretical prediction for producing transversely (dashed) and longitudinally (dash-dotted) polarized $D^*$ mesons, as well as the total decay rate (solid)

are used. The relation to be tested is

$$\frac{\Gamma_L}{\Gamma_T}(\overline{B}^0 \to D^{*+}\rho^-) = \frac{\Gamma_L}{\Gamma_T}(\overline{B}^0 \to D^{*+}\ell^-\overline{\nu}_\ell)\Big|_{q^2=m_\rho^2} . \tag{2}$$

CLEO has new data on the polarization in the $D^{*+}\rho^-$ final state. They measure the polarization of both vector particles. In order to ensure that they can accurately do this, they first measure the polarizations in $D\rho^-$ (see Fig. 3), and also in $D^{*+}\pi^-$ where the $D^{*+}$ must be fully polarized (see Fig. 7(a)). The $cos\theta$ distribution for the $\rho^-$ and the $D^{*+}$ are shown separately in Fig. 7(b), and 7(c), respectively. A simultaneous fit gives a measured

$$\frac{\Gamma_L}{\Gamma_L + \Gamma_T} = (90 \pm 5 \pm 7)\%, \tag{3}$$

close to the 88% predicted.

### 2.3.3 $f_{D_s}$ from factorization in $B$ decay and the CLEO measurement of $\Gamma(D_s^+ \to \mu^+\nu)/\Gamma(D_s^+ \to \phi\pi^+)$

Factorization has been used to estimate the decay constant $f_{D_s}$ using the reaction $\overline{B}^0 \to D^{*+}D_s^-$ and the relationship

$$\frac{\Gamma\left(\overline{B}^0 \to D^{*+}D_s^-\right)}{\frac{d\Gamma}{dq^2}\left(\overline{B}^0 \to D^{*+}l^-\overline{\nu}_\ell\right)\Big|_{q^2=m_{D_s}^2}} = \delta \times 6\pi^2 f_{D_s}^2 |V_{cs}|^2. \tag{4}$$

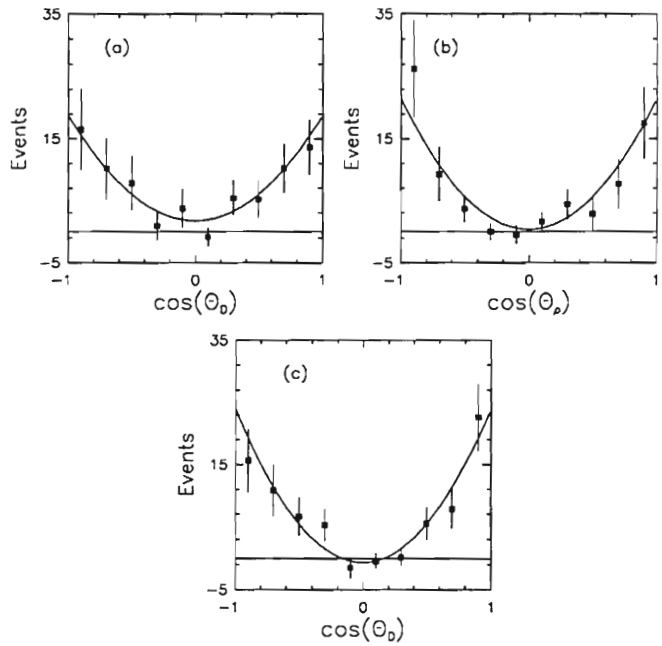


Figure 7: (a) Helicity angle, $\cos\theta$, distributions from $D^{*+} \to D^0\pi^+$ in $\overline{B}^0 \to D^{*+}\rho^-$, (b) $\rho^- \to \pi^-\pi^0$ in $\overline{B}^0 \to D^{*+}\rho^-$, and (c) $D^{*+} \to D^0\pi^+$ in $\overline{B}^0 \to D^{*+}\pi^-$.

where $|V_{cs}| = 0.9744$ and $\delta = 0.41$ [8, 12]. $\delta$ accounts for the fact that the scalar $D_s^-$ forces the $D^{*+}$ into a purely longitudinally polarized state, and also includes a QCD correction. Thus, in vector-pseudoscalar modes, factorization means that the left hand side of equation (4) refers to only the longitudinal part of the semileptonic width. (In the case of $h^- = \pi^-$ the transverse part of the semileptonic width is forced to zero by the extremely low value of $q^2$, equal to $m_\pi^2$.)

Unlike earlier approaches, here I obtain a relationship between the measured two-body hadronic branching ratio and the product $f_{D_s}^2 \cdot \mathcal{B}(D_s^+ \to \phi\pi^+)$. First the measured two-body $B$ branching ratios are needed. These are given in Table 4. These branching ratios use $\mathcal{B}(D_s^+ \to \phi\pi^+) = 3.7\%$, which is based on assuming that the width for $D_s \to \phi\ell\nu$ can be related to $D^+ \to K^*\ell\nu$ with a $\approx$10% correction given by the quark model [15].

We can average in the $D^{*0}$ mode since it must have the same width as the $D^{*+}$ mode by isospin conservation, and the charge and neutral $B$ lifetimes are equal to within $\pm$10% [16]. (Note that $B^- \to D^{*0}D_s^-$ cannot occur via the color suppressed spectator diagram.) Treating $\mathcal{B}(D_s^+ \to \phi\pi^+)$ as an unmeasured parameter, and using

Table 4: $\mathcal{B}(B \to D^* D_s^-)$ for $\mathcal{B}(D_s^+ \to \phi\pi^+) = 3.7\%$

| Mode | Experiment | $\mathcal{B}$ (%) |
|---|---|---|
| $D^{*+}D_s^-$ | CLEO[13] | $1.2 \pm 0.8$ |
| $D^{*+}D_s^-$ | ARGUS[14] | $0.8 \pm 0.6$ |
| $D^{*0}D_s^-$ | ARGUS[14] | $0.8 \pm 0.6$ |
| Average | | $0.9 \pm 0.4$ |

equation (4), results in the relationship

$$f_{D_s} = (288 \pm 64)\sqrt{\frac{3.7\%}{\mathcal{B}(D_s^+ \to \phi\pi^+)}} \text{ MeV}. \tag{5}$$

$f_{D_s}$ is related to the branching ratio of purely leptonic decay modes of the $D_s$ meson and using [17]

$$\Gamma(D_s^+ \to \ell^+\nu) = \frac{1}{8\pi} G_F^2 f_{D_s}^2 m_\ell^2 M_{D_s} \left(1 - \frac{m_\ell^2}{M_{D_s}^2}\right)^2 |V_{cs}|^2 \quad . \tag{6}$$

CLEO has recently measured the width ratio $\Gamma(D_s^+ \to \mu^+\nu)/\Gamma(D_s^+ \to \phi\pi^+) = 0.245 \pm 0.052 \pm 0.074$ [15], which leads to another relationship between $f_{D_s}$ and $\mathcal{B}(D_s^+ \to \phi\pi^+)$:

$$f_{D_s} = (344 \pm 64)\sqrt{\frac{\mathcal{B}(D_s \to \phi\pi^+)}{3.7\%}} \text{ MeV}. \tag{7}$$

Plots of the two relationships are shown in Fig. 8. Solving the two equations gives

$$f_{D_s} = 315 \pm 46 \text{ MeV}, \text{ and } \mathcal{B}(D_s \to \phi\pi^+) = (3.1 \pm 0.9)\%. \tag{8}$$

Another way of gaining information on the product $f_{D_s}^2 \cdot \mathcal{B}(D_s \to \phi\pi^+)$ is to use a theoretical model by Neubert et al. [18], which predicts

$$\frac{\Gamma(\overline{B}^0 \to D^+ D_s^-)}{\Gamma(\overline{B}^0 \to D^+\pi^-)} = 1.03 \left(\frac{f_{D_s}}{f_\pi}\right)^2 . \tag{9}$$

Using the data in Table 5, results in the equation

$$f_{D_s} = (275 \pm 54)\sqrt{\frac{\mathcal{B}(D_s \to \phi\pi^+)}{3.7\%}} \text{ MeV}. \tag{10}$$

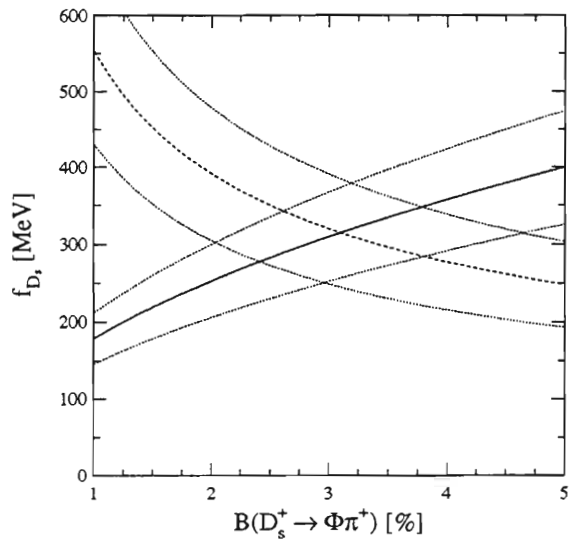


Figure 8: Predictions for $f_{D_s}$ obtained using $B \to D^* D_s^-$ data and the factorization assumption as a function of $\mathcal{B}(D_s^+ \to \phi\pi^+)$ (dashed curve), and the result of the CLEO measurement of $\Gamma(D_s^+ \to \mu^+\nu)/\Gamma(D_s^+ \to \phi\pi^+)$ (solid curve). The parallel top and bottom curves show the one $\sigma$ error limits.

Table 5: $\mathcal{B}(B \to DD_s^-)$ for $\mathcal{B}(D_s^+ \to \phi\pi^+)$=3.7%

| Mode | Experiment | $\mathcal{B}$ (%) |
|---|---|---|
| $D^+D_s^-$ | ARGUS[14] | $1.2 \pm 1.0$ |
| $D^+D_s^-$ | CLEO[13] | $0.6 \pm 0.4$ |
| $D^0D_s^-$ | ARGUS[14] | $1.5 \pm 0.7$ |
| $D^0D_s^-$ | CLEO[13] | $1.6 \pm 0.9$ |
| Average | | 1.0±0.3 |

As the 275 MeV is quite similar to the 288 MeV in equation (5), the model is in good agreement with the factorization test, and supports a large value of $f_{D_s}$.

A large value of $f_{D_s}$ is particularly important for the future study of CP violation in $B$ decays. Fig. 9 shows the information available about the CKM parameters $\rho$ and $\eta$ (in the Wolfenstein formulation) [19], for three values of the top quark mass, one close to the CDF lower limit, one close to the upper limit from radiative corrections and one in the middle [20]. The semicircle centered at $(\rho, \eta)$ equals (0,0) comes from the CLEO measurement of $V_{ub}/V_{cb}$ [2]. The narrow, almost horizontal, band comes from the measurement of $\epsilon$ in $K_L^0$ decay, and the circular arcs centered at (1,0) come

from $B^0 - \overline{B}^0$ mixing [23]. These later radii depend on the value of $f_B$, where the leftward curve is for $f_B$= 160 MeV, and the rightmost for $f_B$=240 MeV; these values are given by the allowed range of lattice gauge calculations [21]. The calculations seem to be underestimating the value of $f_{D_s}$, and therefore large values of $f_B$ are favored. Consider the middle plot, that for $m_t$=140 MeV. Here the triangle shows the CP violating angles. The one with a vertex at (1,0) can be measured with the $\psi K_s$ mode. A value of $f_B$ larger than the lattice gauge estimates increases this angle toward $45^0$, which gives the maximal amount of CP asymmetry.

## 2.4 Spin Symmetry Tests

In heavy quark effective theory (HQET), the magnetic moment of the heavy quark doesn't play any role in the lowest order calculation [22]. This leads to the prediction that the width for $D^+h^-$ will be equal to the width for $D^{*+}h^-$, except for corrections due to the particle masses. The results, summarized in Table 6, are consistent with this hypothesis.

Table 6: Tests of Spin Symmetry

| $\Gamma(D^{*+}h^-)/\Gamma(D^+h^-)$ | Value | Group | Theory | Author |
|---|---|---|---|---|
| $h^- = \pi^-$ | 1.2±0.3 | CLEO | 0.97 | Neubert [18] |
| $h^- = \rho^-$ | 1.2±0.3 | CLEO | 1.12 | Neubert [18] |
| $h^- = D_s^-$ | 0.9±0.5 | CLEO& ARGUS | 0.73 | Rosner [12] |

## 2.5 Color Suppression

### 2.5.1 Explict search for color suppressed modes

CLEO has done an explicit search for modes, other than those containing charmonium, which can only occur via the color suppressed diagram shown in Fig. 1(b). No positive signals were found. The upper limits are given in Table 7 and are compared to prediction of the BSW [24] and the RI models [11]. Both models are based on factorization. The BSW model will be discussed in the next section. The RI model uses heavy quark symmetry [22] to find the form-factors for the $B \to D$ amplitude, and

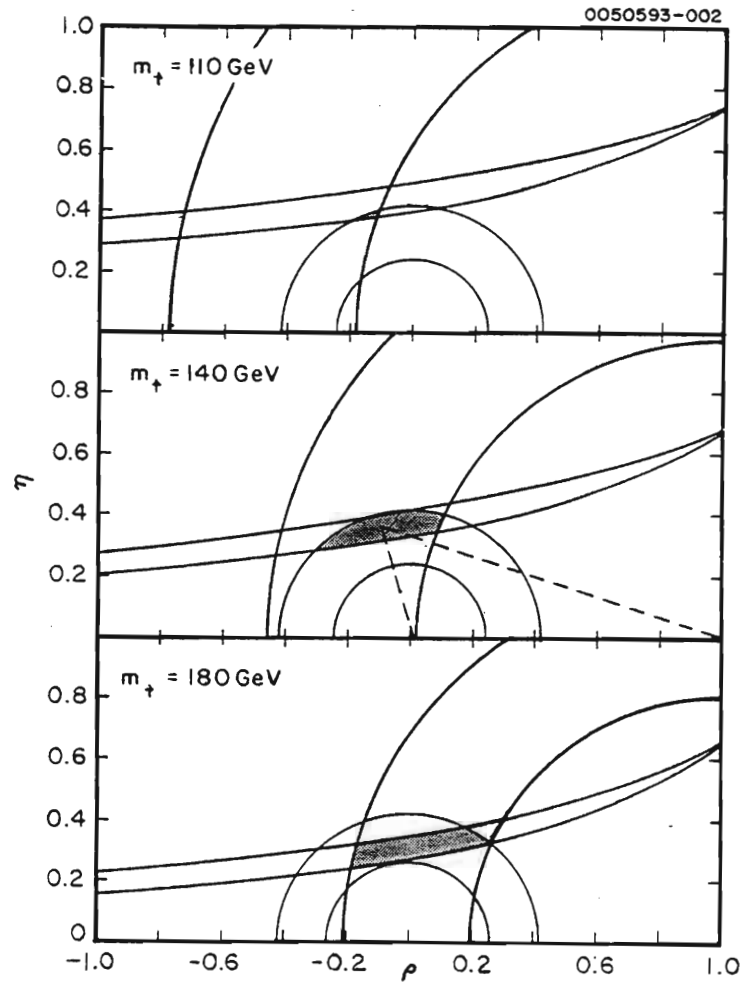


Figure 9: Allowed regions in the $\rho - \eta$ plane in the Standard Model. The arc centered on (1,0) come form measurements of $B^0 - \overline{B}^0$ mixing; the leftward arc is for $f_B$=160 MeV and the rightward one is for $f_B$=260 MeV. the two close to horizontal curves come from the $\epsilon$ measurement in $K_L^0$ decays, where $B_K$ is taken to vary from 0.55 to 0.83. The semicircles centered at the origin come from a recent CLEO result of $V_{ub}/V_{cb} = 0.075 \pm 0.020$. The allowed regions are shaded.

$\tau^-$ decay data are used to find the hadronic currents associated with the virtual $W$. The data do not yet have the sensitivity to reach the level of the model predictions.

### 2.5.2 Determination of the BSW parameters $a_1$ and $a_2$

Let us consider again the diagrams presented in Fig. 1. BSW assign two parameters, $a_1$ and $a_2$ to describe these diagrams. These parameters can be calculated in QCD in terms of the coefficients $c_+$ and $c_-$ and the "color matching" factor $\xi$, which is 1/3

Table 7: Branching ratios of color suppressed $B$ decays and comparisons with models.

| Decay Mode | U. L. (%) | BSW (%) | $\Gamma$ (BSW) | RI model(%) |
|---|---|---|---|---|
| $\overline{B}^0 \to D^0\pi^0$ | $< 0.035$ | 0.009 | $0.201a_2^2$ | $0.0013 - 0.0018$ |
| $\overline{B}^0 \to D^0\rho^0$ | $< 0.042$ | 0.006 | $0.136a_2^2$ | 0.00044 |
| $\overline{B}^0 \to D^0\eta$ | $< 0.075$ | | | |
| $\overline{B}^0 \to D^0\eta'$ | $< 0.080$ | 0.00205 | $0.03a_2^2$ | |
| $\overline{B}^0 \to D^0\omega$ | $< 0.048$ | 0.005 | $0.06a_2^2$ | |
| $\overline{B}^0 \to D^{*0}\pi^0$ | $< 0.071$ | 0.009 | $0.213a_2^2$ | $0.0013 - 0.0018$ |
| $\overline{B}^0 \to D^{*0}\rho^0$ | $< 0.099$ | 0.010 | $0.223a_2^2$ | $0.0013 - 0.0018$ |
| $\overline{B}^0 \to D^{*0}\eta$ | $< 0.094$ | 0.0058 | $0.07a_2^2$ | |
| $\overline{B}^0 \to D^{*0}\eta'$ | $< 0.37$ | 0.0033 | $0.04a_2^2$ | |
| $\overline{B}^0 \to D^{*0}\omega$ | $< 0.15$ | 0.026 | $0.31a_2^2$ | |

for 3 colors. The $c's$ can be calculated in the "leading log" approximation using

$$c_- = \frac{1}{c_+^2} = \left[\frac{\alpha_s(m_c)}{\alpha_s(M_W)}\right]^{\frac{12}{(33-2N_f)}}, \tag{11}$$

where $N_f$ is the number of active quark flavors (4). BSW define $a_1$ and $a_2$ as

$$2a_1 = c_+ + c_- + (c_+ - c_-)\xi, \; 2a_2 = c_+ - c_- + (c_+ + c_-)\xi. \tag{12}$$

BSW use the data to find $a_1$ and $a_2$, and use these relationships to infer a value of $\xi$. In this model the wave-function overlap between the $c$-quark from the $b$-quark decay and the spectator antiquark must be calculated for every decay mode. If both diagrams are allowed this calculation must be done for each piece that multiplies $a_1$ or $a_2$. Finally, the model predicts widths so the lifetimes enter. The branching ratios quoted above are based on the assumption that $\Upsilon(4S)$ decays half into $B^0\overline{B}^0$ and half into $B^+B^-$. Even though the charged, $f_-$, and neutral $B$, $f_0$, fractions have not been directly measured on the $\Upsilon(4S)$, one important ratio has been measured. I use the new CLEO II experimental value [25]

$$\frac{f_-\tau^-}{f_0\tau_0} = \frac{\Gamma(B \to D^{*0}\ell\overline{\nu}_\ell)}{\Gamma(B \to D^{*+}\ell\overline{\nu}_\ell)} = 1.2 \pm 0.2 \pm 0.2, \tag{13}$$

where $\tau^-$ and $\tau^0$ refer to the respective charged and neutral $B$ lifetimes. It is particularly important to use this measured value when deriving the ratio $a_2/a_1$ (see below).

A fit to the $D^{*+}\pi^-$, $D^{*+}\rho^-$, $D^+\pi^-$, and $D^+\rho^-$, CLEO branching ratios yields

$$a_1 = 1.07 \pm 0.04 \pm 0.03 \pm 0.09, \tag{14}$$

where the first two errors come from the statistical and systematic errors on the branching ratios, and the third error comes from the error on the ratio $f_-\tau^-/f_0\tau_0$.

To determine $a_2$ the decays to charmonium are used as they are the only final states thus far found in purely color suppressed modes. The new CLEO branching ratios for these modes are listed in Table 8. The PDG values are used for the $\psi \to \ell^+\ell^-$ branching ratios [9].

Table 8: Exclusive charmonium branching ratios

| Mode | $\mathcal{B}$ (%) |
|---|---|
| $B^- \to \psi K^-$ | $0.112 \pm 0.015 \pm 0.009$ |
| $\overline{B}^0 \to \psi K^0$ | $0.06 \pm 0.02 \pm 0.01$ |
| $B^- \to \psi K^{*-}$ | $0.16 \pm 0.05 \pm 0.02$ |
| $\overline{B}^0 \to \psi K^{*0}$ | $0.15 \pm 0.03 \pm 0.02$ |
| $B^- \to \psi' K^-$ | $<0.09$ |
| $\overline{B}^0 \to \psi' K^0$ | $0.06 \pm 0.02 \pm 0.01$ |
| $B^- \to \psi' K^{*-}$ | $<0.48$ |
| $\overline{B}^0 \to \psi' K^{*0}$ | $0.14 \pm 0.06 \pm 0.04$ |
| $B^- \to \chi_{c1} K^-$ | $0.14 \pm 0.06 \pm 0.02$ |

A fit to the $\psi K$ and $\psi K^*$ final states gives

$$a_2 = 0.27 \pm 0.01 \pm 0.01 \pm 0.02, \tag{15}$$

where the sources of error are the same as for the $a_1$ case.

The above techniques give values for $a_1$ and $a_2$ but not the relative sign between them. In modes where both diagrams can contribute, there is an interference between the diagrams and the relative sign can be determined. Two-body $B^-$ decays to a $D^{0(*)}$ and $\pi^-$ or $\rho^-$, involve both diagrams. The ratio of branching ratios for each set of charge analogue channels for $B^-/\overline{B}^0$ gives a value for $a_2/a_1$. A fit to the four distinct ratios listed in Table 9 gives

$$a_2/a_1 = +0.20 \pm 0.03 \pm 0.02 \pm 0.10, \tag{16}$$

Table 9: Predicted versus measured ratios

| $\frac{\Gamma(B^-)}{\Gamma(\overline{B}^0)}$ | BSW | $a_2/a_1$ =-0.24 | $a_2/a_1$ =+0.24 | Measured | RI model |
|---|---|---|---|---|---|
| $D^0\pi^-/D^+\pi^-$ | $(1+1.23a_2/a_1)^2$ | 0.50 | 1.68 | $2.1 \pm 0.3 \pm 0.4$ | 1.20-1.28 |
| $D^0\rho^-\ D^+\rho^-$ | $(1+0.66a_2/a_1)^2$ | 0.71 | 1.34 | $1.7 \pm 0.3 \pm 0.3$ | 1.09-1.12 |
| $D^{*0}\pi^-/D^{*+}\pi^-$ | $(1+1.29a_2/a_1)^2$ | 0.48 | 1.72 | $1.9 \pm 0.2 \pm 0.1$ | 1.19-1.27 |
| $D^{*0}\rho^-/D^{*+}\rho^-$ | $(1+1.50a_2/a_1)^2$ | 0.41 | 1.85 | $1.9 \pm 0.2 \pm 0.1$ | 1.10-1.36 |

where the errors are as stated above for $a_1$ or $a_2$, separately.

This result has a positive value for the relative sign which is revealed quite clearly in Table 9. In the columns labeled with negative and positive values of $a_2/a_1$, the decay width ratios are computed using the BSW predictions, where the absolute value of $a_2/a_1$ is fixed to 0.24 as determined from the values of $a_1$ and $a_2$ found separately above. In all cases the measured ratios are consistent with the positive value and inconsistent with the negative value. Also shown for comparison are the predictions of the RI model, which seem somewhat low.

In charm decays the $a_2/a_1$ ratio is negative showing a destructive interference between the color suppressed and non-suppressed diagrams and possibly providing an explanation for why the $D^+$ total width is $\approx$2.5 times lower than $D^0$ or $D_s^+$ [26]. In the $B$ case we see that the interference is constructive which tends to increase the $B^-$ width relative to the $\overline{B}^0$. In the charm case low multiplicity modes form a much larger fraction of the decay width than in beauty decays. Thus we expect the $B^-$ lifetime to be somewhat less than the $\overline{B}^0$ lifetime, but not by the large factor present in the charm case.

### 2.5.3 Polarization of the $\psi K^*$ final state

The vector-vector final state $\psi K^*$ can be useful for studies of CP violation if it polarized predominantly in either the longitudinal or the in transverse mode. CLEO has measured this polarization and finds $\Gamma_L/\Gamma = 0.84 \pm 0.06 \pm 0.08$. Therefore, this mode will be useful for measuring CP violation. This is consistent with a previous result from ARGUS [27].

## 2.6 $D^{**}$ Final States

Thus far I have discussed the cases where the $c$-quark from the $b$-quark decay forms either a $D$ or $D^*$ meson with the spectator anti-quark. In this situation the orbital angular momentum, $L$, is zero between the $c$-quark and the antiquark. Other resonant systems of higher mass are predicted to exist. Four states should exist in the case where $L = 1$, two of which have been discovered. These are a $1^+$ state at a nominal mass of 2420 MeV, which decays into $D^*\pi$ and a $2^+$ state at 2460 MeV, which decays mostly into $D\pi$ but also into $D^*\pi$.

An extensive search for two-body decays into the known $1^+$ and $2^+$ states and a $\pi^-$ or $\rho^-$ has been performed by CLEO. ARGUS has also looked for the $D^{**}(2420)\pi^-$ final state using a partial reconstruction technique, and quote a branching ratio of $(30\pm10)\times10^{-4}$[28]. The results are given in Table 10. To determine the branching ratios, CLEO uses $\mathcal{B}(D^{**0}(2420) \to D^{*+}\pi^-)$ equal to 67%, from isospin conservation, and $D^{**0}(2460)$ decays into $D^{*+}\pi^-$, and $D^+\pi^-$ as 20%, and 30%, respectively.

The CLEO data are shown in Fig. 10, for the $D^{*+}\pi^-$ final state of the $D^{**}$'s. Signals in one final state, $D^{**0}(2420)\pi^-$ are clearly seen by both groups, although the CLEO branching ratio is 2.5 times smaller than ARGUS. The CLEO data also show hints of signals in the other modes. Both the Bari [29] model and the RI [11] model are based on factorization and seem to be consistent with the data.

Table 10: CLEO II Branching Ratio for $B \to D^{**}(n\pi)$.

| Modes | $\mathcal{B}$ | Bari model [29] | RI model [11] |
|---|---|---|---|
| $D^{**0}(2420)\pi^-$ | $(12\pm5\pm4\pm3)\times10^{-4}$ | $4 \times 10^{-4}$ | $(7.5\text{-}13)\times10^{-4}$ |
| $D^{**}(2460)\pi^-$ | | $6 \times 10^{-4}$ | $(5\text{-}8)\times10^{-4}$ |
| $(D^{**0} \to D^{*+}\pi^-)$ | $< 2.7 \times 10^{-3}$ | | |
| $(D^{**0} \to D^{+}\pi^-)$ | $< 1.5 \times 10^{-3}$ | | |
| $D^{**0}(2420)\rho^-$ | $< 1.7 \times 10^{-3}$ | $1 \times 10^{-3}$ | $(13\text{-}24)\times10^{-4}$ |
| $D^{**0}(2460)\rho^-$ | $< 5 \times 10^{-3}$ | $1 \times 10^{-3}$ | $(10\text{-}20)\times10^{-4}$ |

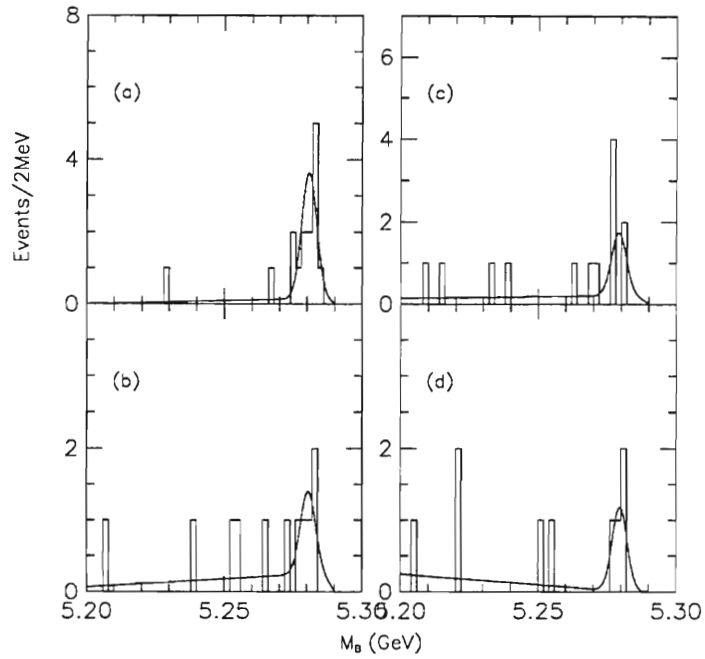


Figure 10: $B$ candidate mass distributions for (a) $D^{**0}(2420)\pi^-$, (b)$D^{**0}(2460)\pi^-$, (c)$D^{**0}(2420)\rho^-$, (d)$D^{**0}(2460)\rho^-$. In all cases $D^{**0}(2420) \to D^{*+}\pi^-$. The curves are fits to a signal Gaussian and a background shape consisting of a linear piece coupled with a parabolic falloff near threshold.

# 3 Conclusions

Factorization in two-body decays, first checked by Bortoletto and Stone [8], still works extremely well for the $D^{*+}\pi^-$ and $D^{*+}\rho^-$ final states. Even the polarization in the later is the same as that expected in semileptonic decays. Much more precise two-body branching ratios from CLEO have shown that the interference between the color suppressed and non-color suppressed diagrams is constructive, opposite to what occurs in charm decay. The $D^{**0}(2420)\pi^-$ final state has been seen clearly by both ARGUS and CLEO for the first time. Combining factorization with the CLEO measurement of $\Gamma(D_s^+ \to \mu^+\nu)/\Gamma(D_s^+ \to \phi\pi^+)$, gives $f_{D_s} = 315 \pm 46$ MeV, and $\mathcal{B}(D_s \to \phi\pi^+) = (3.1 \pm 0.9)\%$. The sum of exclusive hadronic channels seen so far in $B^-$ decays is only about 6% (and is lower in $\overline{B}^0$ decays). Therefore, there are many more decays to see and much work needs to be done.

I thank many members of the CLEO and ARGUS collaborations for useful dis-

cussions. Especially helpful in preparing this document were M. Artuso, T. Browder, K. Honscheid, G. Moneti, F. Muheim, W. Ross, S. Schrenk and G. Zhu. This work was supported by the National Science Foundation.

# References

[1] N.G. Desphande, "Theory of Penguins in $B$ Decays," in $B$ **Decays**, ed. by S. Stone, World Scientific, Singapore (1991).

[2] R. Poling, "Semileptonic $B$ Decays," in these procedings.

[3] F. Butler et al. (CLEO), Phys. Rev. Lett. **69**, 2041 (1992).

[4] When calculating B branching fractions using the $D^0 \to K^-\pi^+$ and $D^+ \to K^-\pi^+\pi^+$ decay modes, the systematic error from the tracking efficiency is included in the systematic error on the B branching fraction. To avoid counting this systematic error twice, CLEO uses the values of $\mathcal{B}(D^0 \to K^-\pi^+) = (3.91 \pm 0.08 \pm 0.07)\%$ and $\mathcal{B}(D^+ \to K^-\pi^+\pi^+) = (10.0 \pm 1.0 \pm 1.0)\%$ which do not include the tracking systematic error.

[5] S. Behrends et al. (CLEO), Phys. Rev. Lett. **50**, 881 (1983); H. Albrecht et al. (ARGUS), Zeit. Phys. C **48**, 543 (1990); D. Bortoletto et al. (CLEO), Phys. Rev. D **45**, 21 (1992).

[6] J. Bjorken, Nucl. Phys. B (Proc. Suppl) **11**, 325 (1989).

[7] M. J. Dugan and B. Grinstein, Phys. Lett. B **255**, 583 (1991); and references therein.

[8] D. Bortoletto and S. Stone, Phys. Rev. Lett. **65**, 2951 (1990).

[9] K. Hikasa et al., (Particle Data Group) Phys. Rev. D **45**, 1 (1992).

[10] X. Y. Pham, X. C. Vu, Phys. Rev. D **46**, 261 (1992).

[11] C. Reader and N. Isgur, Phys. Rev. D **47**, 1007 (1993).

[12] J. L. Rosner, Phys. Rev. D **42**, 3732 (1990).

[13] D. Bortoletto et al. (CLEO), Phys. Rev. Lett. **226**, 192 (1989).

[14] H. Albrecht et al (ARGUS), Zeit. Phys. C **54**, 1 (1992); H. Albrecht et al (ARGUS), Phys. Lett. B **187**, 425 (1987).

[15] D. Acosta, et al. (CLEO), "First Measurement of $\Gamma(D_s^+ \to \mu^+\nu)/\Gamma((D_s^+ \to \phi\pi^+)$", CLNS 93/1238 (1993).

[16] D. Karlen, "B Hadron Lifetimes," in these procedings.

[17] J. L. Rosner, in **Particles and Fields 3**, Proceed. of the 1988 Banff Summer Inst., Banff, Alberta, Canada, ed. by A. N. Kamal and F. C. Khanna, World Scientific, Singapore, 395 (1989).

[18] M. Neubert, V. Riekert, Q. P. Xu and B. Stech in *Heavy Flavours*, edited by A. J. Buras and H. Lindner (World Scientific, Singapore, 1992).

[19] L. Wolfenstein, Phys. Rev. D **31**, 2381 (1985).

[20] W. Marciano, "Status of CKM Constraints," in these procedings.

[21] G. Martinelli "Heavy Flavour on the Lattice: Results and Prospects," in these proceedings; C. Bernard et al., "A Lattice Computation of the Decay Constants of $B$ and $D$ Mesons", BNL preprint 49068 (1993).

[22] N. Isgur and M. B. Wise, Phys. Lett. B **232**, 113 (1989); ibid, **B237**, 527(1990), and references contained therein.

[23] The formulas used for these curves is given in A. J. Buras and M. K. Harlander, "A Top Quark Story: Quark Mixing, CP Violation and Rare Decays in the Standard Model," in **Heavy Flavours**, ed. by A. J. Buras and M. Lindner, World Scientific, Singapore (1992).

[24] M. Bauer, B. Stech, and M. Wirbel, Zeit. Phys. C **29**, 637 (1985); *ibid* **34**, 103 (1987); *ibid* **42**, 671 (1989).

[25] D. S. Akerib et al.(CLEO), "The Ratio $\Gamma(B^- \to D^{*0}\ell^-\bar{\nu})/\Gamma(\overline{B}^0 \to D^{*+}\ell^-\bar{\nu})$, submitted to Int. Europhysics Conf. on High Energy Physics, Marseille, France (1993).

[26] B. Guerina, S. Nussinov, R. D. Peccei and R. Rückl Phys. Lett. B **89**, 111 (1979).

[27] M. Danilov, "Heavy Flavour Physics," in Proc. of Joint Int. Lepton- Photon Symp. and Europhysics Conf. on HEP, Geneva, 1991, ed. S. Hegarty, K. Potter, E. Quercigh, World Scientific, Singapore (1992).

[28] P. Krieger, "Analysis of $B^- \to D^{**0}(2420)\pi^-$," in these proceedings.

[29] P. Colangelo, G. Nardulli, N. Paver, Phys. Lett. B **303**, 152 (1993).